

DNA and HSA interaction of Vanadium (IV), Copper (II), and Zinc (II) complexes derived from an asymmetric bidentate Schiff-base ligand: multi spectroscopic, viscosity measurements, molecular docking, and ONIOM studies

Monireh Dehkhodaei¹ · Mehdi Sahihi¹ · Hadi Amiri Rudbari¹ · Fariborz Momenbeik¹

Received: 14 May 2017 / Accepted: 28 October 2017
© SBIC 2017

Abstract The interaction of three complexes [Zn(II), Cu(II), and V(IV)] derived from an asymmetric bidentate Schiff-base ligand with DNA and HSA was studied using fluorescence quenching, UV–Vis spectroscopy, viscosity measurements, and computational methods [molecular docking and our Own N-layered Integrated molecular Orbital and molecular Mechanics (ONIOM)]. The obtained results revealed that the DNA and HSA affinities for binding of the synthesized compounds follow as V(IV) > Zn(II) > Cu(II) and Zn(II) > V(IV) > Cu(II), respectively. The distance between these compounds and HSA was obtained based on the Förster's theory of non-radiative energy transfer. Furthermore, computational molecular docking was carried out to investigate the DNA- and HSA-binding pose of the compounds. Molecular docking calculations showed that H-bond, hydrophobic, and π -cation interactions have dominant role in stability of the compound–HSA complexes. ONIOM method was utilized to investigate the HSA binding of the compounds more precisely in which molecular-mechanics method (UFF) and semi-empirical method (PM6) were selected for the low layer and the high layer, respectively. The results show that the structural parameters of the compounds changed along with binding, indicating the strong interaction between the compounds with HSA and

DNA. Viscosity measurements as well as computational docking data suggest that all metal complexes interact with DNA, presumably by groove-binding mechanism.

Keywords DNA interaction · HSA binding · Schiff base · Molecular docking · ONIOM

Introduction

Schiff-base ligands and their metal complexes have been studied increasingly in past decades. These compounds show wide variety of chemical structures with different physicochemical properties [1–4]. On the other hand, there are many reports in the literatures based on their potential applications in different sciences, e.g., solar cells, molecular recognition, catalysis, and nano-materials, due to mild reaction conditions and high synthesis rates of Schiff-base complexes [5–8]. In addition, in the recent years, remarkable attention has been paid to the biological applications of Schiff-base compounds due to their stability, biocompatibility, and biological activities [9]. Biochemists believe that the imine group existence in the chemical structure of Schiff bases is the main cause of their biological activity of Schiff-base compounds. Furthermore, complexation of Schiff-base ligands with transition metal ions enhances their biological activities [10–12]. In addition, metal ion compounds are attractive candidates in biological fields and medicinal applications. The role of Copper(II) as anti-tumor and antibacterial agent [13, 14], Vanadium (IV) as antitumor, antimicrobial, an insulin-mimetic, and antidiabetic agent [15–17] and Zinc (II) in peptidase enzymes, its antimicrobial activity, its function as enzyme activator or inhibitor, and its partnership in intracellular and intercellular signal transduction [18–20] are the best examples

Electronic supplementary material The online version of this article (<https://doi.org/10.1007/s00775-017-1505-9>) contains supplementary material, which is available to authorized users.

✉ Mehdi Sahihi
m.sahihi@chem.ui.ac.ir

✉ Hadi Amiri Rudbari
hamiri1358@gmail.com; h.a.rudbari@sci.ui.ac.ir

¹ Department of Chemistry, University of Isfahan, Isfahan 81746-73441, Iran

for biological importance of these metal ions. Therefore, studying the interaction of Schiff-base metal complexes with biomacromolecules such as DNA and proteins is the first step for the intellectual design and fabrication of new and more efficient pharmaceutical molecules.

Proteins and DNA are vital members of our life and the major target in medicine and pharmacy fields. In general, proteins are known as the major targets for most of the drugs in organisms [21]. The interaction mechanism of a drug with plasma proteins is key point to understand its pharmacodynamics and pharmacokinetics [22]. Their interaction with drugs has great influence on drug absorption/distribution in the circulatory system [23] and can prevent rapid elimination of drug from blood stream [24]. Human serum albumin (HSA) is the most abundant plasma protein. In addition, it is known as the dominant transporter plasma protein for endogenous and exogenous ligands (e.g. fatty acids and hormones) [25] and is one of the most important targets in binding of various drugs (e.g. warfarin, diazepam, and ibuprofen) [26] and metal ions [27]. The HSA binding of a drug increases its solubility in plasma, decreases its toxicity, protects it from oxidation, prolongs its in vivo half-life, and increases its pharmaceutical effect [28–31]. Understanding of these interaction mechanisms helps us to know the pharmacodynamics and pharmacokinetics effects of drugs.

In addition, regarding DNA as one of the first targets of intracellular anticancer drugs, investigation of metal complexes interactions with this double helix is key stage in the design of new drugs with anticancer activities [32, 33].

Herein, the Fish Sperm DNA (FS-DNA)- and HSA-binding of the Vanadium (IV), Copper (II), and Zinc (II) complexes derived from an asymmetric bidentate Schiff-base ligand, which have been synthesized in our research group earlier [34], have been evaluated using both experimental (fluorescence quenching, UV–Vis spectroscopy and viscosity measurements) and computational methods (molecular docking and ONIOM).

Experimental section

Chemicals and instrumentation

HSA and DNA were purchased from Sigma-Aldrich. Other chemicals were purchased from Merck and were used without further purification. Buffer solutions were prepared using analytical grade salts and double distilled water. All the solutions were used freshly after preparation. The UV–Vis spectra were recorded by Shimadzu UV-160 spectrophotometer. Fluorescence and Viscosity measurements were carried out at room temperature using Shimadzu RF-5000 spectrofluorometer and a Brookfield rotational viscometer, respectively.

HSA- and DNA-binding experiments

Preparation of the complexes, and HSA and DNA stock solutions

A stock solution of HSA was prepared by dissolving the desired amount of HSA in 50 mM phosphate buffer (pH = 7). The HSA stock solution was stored at 4 °C in dark and was used within 2 h. HSA concentration was determined using UV–Vis spectrophotometry and the molar absorption coefficient $35,700 \text{ M}^{-1} \text{ cm}^{-1}$ at 278 nm [35]. The stock solution of FS-DNA was prepared in 50 mM Tris buffer at pH = 7.5 and was stored at 4 °C. The FS-DNA concentration per nucleotide was determined using absorption intensity at 260 nm after adequate dilution with the buffer and using the reported molar absorptivity of $6600 \text{ M}^{-1} \text{ cm}^{-1}$ [36]. Purity of FS-DNA solution was confirmed by ratio of UV absorbance at 260 and 280 nm ($A_{260}/A_{280} = 1.9$), indicating that FS-DNA is free from protein impurity [37]. Also, the stock solutions of the complexes were prepared in dimethylformamide (DMF) and then were diluted to the desired concentrations with corresponding buffer. The volume of DMF in all final solutions was less than 0.5% (v/v), so the effect of DMF was negligible.

Fluorescence spectroscopy measurements

Fluorescence spectroscopy is a sensitive and effective method to study binding of drugs to biomacromolecules. Fluorescence quenching experiment can help us to obtain the binding mode, binding constants, number of binding sites, and intermolecular distances [38]. The interactions of HSA and DNA with the synthesized Schiff-base complexes [Zn(II), Cu(II) and V(IV) complexes] were investigated using fluorescence quenching experiment. Quartz cuvette with 1 cm optical path length was used, and the excitation and emission slits were set at 5 and 10 nm, respectively. In HSA-binding experiments, 2 ml of HSA solution (5 μM) was placed into the cell and various amounts of the complexes solutions (0–50 μM) were added to it. The fluorescence emission spectra were recorded using 295 nm as excitation wavelength and 300–450 nm as emission wavelength range. Although fluorescence of proteins is due to the presence of three amino acids, i.e., tryptophan (Trp), tyrosine (Tyr), and phenylalanine (Phe) residues, the intrinsic fluorescence of HSA comes from tryptophan [39].

In addition, to investigate the binding of the complexes with DNA, the FS-DNA solution was stirred with ethidium bromide (EtBr) with molar ratio of DNA:EtBr 10:1 for 1 h at 4 °C. Significant increase of fluorescence intensity of EtBr is observed at the presence of FS-DNA due to intercalation of the EtBr molecules into the double helix of DNA [40–43]. Then, various amounts of the metal complexes (0–250 μM)

were added to this mixture. The fluorescence spectra were recorded in the range of 500–700 nm with excitation wavelength of 520 nm. The mixture was allowed to incubate for 2 min after addition of the complexes (Scheme 1).

Moreover, in all the HSA- and DNA-binding experiments, the measured fluorescence intensities were corrected for the dilution and the inner filter effect.

UV–Vis absorption spectroscopy measurements

Electronic absorption spectroscopy is one of the used methods for studying the binding affinity. To confirm the binding of the complexes to HSA and DNA, absorption titration experiments were carried out at room temperature. The UV–Vis absorption spectra of the metal complexes' solutions (10 μ M) in the absence and presence of various amounts of HSA and FS-DNA (0–50 μ M) were recorded. In all the measurements, the mixture was allowed to incubate for 2 min before recording the related spectra. Absorption curves of complexes–biomacromolecule mixtures were corrected for both absorptions of biomacromolecule solutions and the dilution effect.

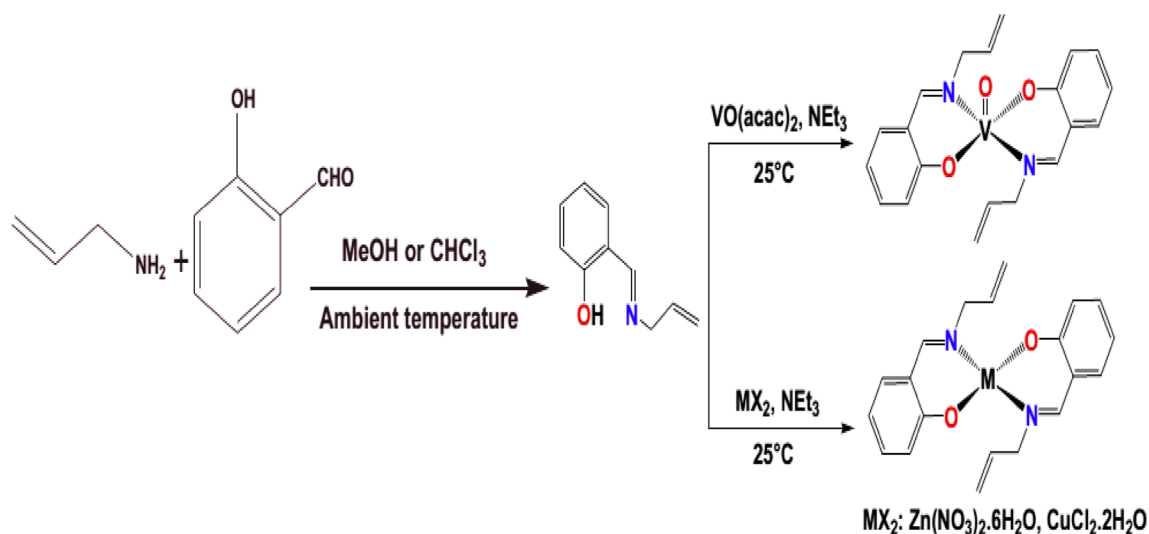
Viscosity measurements

Viscosity experiments were carried out by a rotational viscometer and the measurements were performed at 200 rpm at room temperature. The viscosity of FS-DNA solution was measured in the presence of increasing amounts of the metal complexes. The obtained data are presented as $(\eta/\eta_0)^{1/3}$ versus $[\text{complex}]/[\text{DNA}]$, where η_0 and η are the viscosities of FS-DNA in the absence and presence of the metal complexes, respectively.

Molecular docking procedure

Studying the interaction between drug molecules and bio-macromolecules is one of the interesting topics in biochemistry [44]. Molecular docking is one of the known theoretical techniques for the prediction of interaction between drugs and biomacromolecules. To dock our complexes to HSA and DNA, the 3D structures of the metal complexes were obtained using the .cif files of their X-ray crystal structures [34]. The .cif files were converted to .pdb format using the Mercury software (<http://www.ccdc.cam.ac.uk/>). The crystal structure of HSA (PDB ID: 1AO6) and DNA (PDB ID: 423D) with sequence d(ACCGACGTCGGT)₂ were taken from the Brookhaven Protein Data Bank (<http://www.rcsb.org/pdb>). The resolution of these files was 2.6 and 1.6 Å for HSA and DNA, respectively. Water molecules were deleted from the .pdb files and missing hydrogen atoms were added. Flexible-ligand docking was carried out by AutoDock 4.2.5.1 molecular docking program using the implemented empirical free energy function and the Lamarckian Genetic Algorithm (LGA) [45]. The Gasteiger charges were added to the macromolecule input file and the AutoGrid was used to calculate grids. For docking of the synthesized metal complexes to HSA, the grid box was centred on C $_{\alpha}$ of the Trp-214 residue of protein. Ninety lattice points along X, Y, and Z axes were selected to find the active site of complexes on HSA with a grid point spacing of 0.375 Å.

For the docking of metal complexes with DNA, in the first step, a blind docking with 126 lattice points along X, Y, and Z axes was performed to find the binding site of complexes on DNA with a grid point spacing of 0.375 Å. In the next step, the centre of the grid box was located at the binding site and the second docking was performed using a cubic



Scheme 1 Synthetic routes for the preparation of the complexes

box with $60 \times 60 \times 60$ dimensions. Two hundred and fifty docking runs with 25,000,000 energy evaluations for each run were performed.

Quantum mechanical/molecular-mechanics (QM/MM) calculations

QM/MM calculations were used to investigate the conformational changes on interaction of the complexes with HSA and DNA. To carry out QM/MM calculations, Our own N-layered Integrated molecular Orbital and molecular Mechanics (ONIOM) methodology was employed. The ONIOM can be considered as a hybrid method including quantum mechanical method (QM) and a molecular mechanics (MM). Although this method was used as a two-layer QM/MM in this study, it is capable for combining any number of molecular orbital and molecular-mechanics methods [46]. Using this, method one is also able to apply different ab initio or semi-empirical methods to different parts of a molecule/system. This resulted in producing reliable geometry and energy data at reduced computational time [47].

Real system contains full geometry of the molecule which is considered as MM layer, while the model system contains the chemically most important (core) part of the system is considered as QM layer.

In current work, a two-layer QM/MM method was opted for all calculations. Molecular-mechanics method (UFF) was applied to HSA or DNA as low layer. In similar way, semi-empirical method (PM6) was selected for the complexes as high layer.

Results and discussion

Fluorescence spectroscopy

Figures 1, 2 show the fluorescence quenching of HSA and DNA (5×10^{-6} M) at the presence of various amounts of the complexes, respectively. The fluorescence intensity of protein was quenched through the addition of the complexes. This implies that the complexes strongly interact with HSA, leading to microenvironment changes around the Trp-214 residue. In addition, these complexes can displace EtBr by changing the DNA conformation. Consequently, the DNA-bound EtBr molecules are converted to their free form in solution and cause fluorescence quenching [48, 49].

To determine the binding ability of the complexes, the Stern–Volmer quenching plot (Eq. 1) was obtained by monitoring the fluorescence quenching of HSA and DNA–EtBr with increasing the concentration of the complexes [50]:

$$\frac{F_0}{F} = 1 + K_{sv}[Q] = 1 + k_q\tau[Q], \quad (1)$$

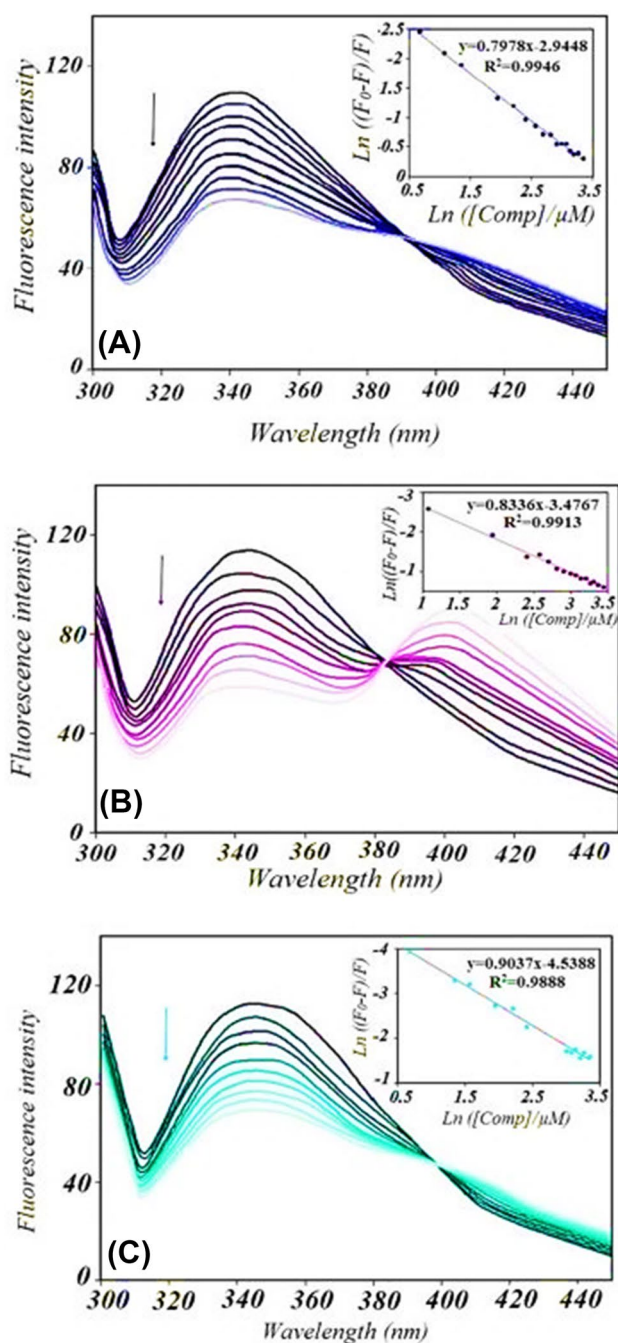


Fig. 1 Fluorescence emission spectra of HSA upon its titration with various amounts of metal complex: **a** Zn(II), **b** V(IV), **c** Cu(II). [HSA] = $5 \mu\text{M}$, [Comp] = 0–50 μM , λ_{ex} = 295 nm

where F_0 and F are the fluorescence intensity of HSA or DNA–EtBr in the absence and presence of the compounds. K_{sv} is the Stern–Volmer quenching constant, k_q is the quenching rate constant of biomolecule, $[Q]$ is concentration of the quencher (complexes), and τ is the average lifetime of biomolecule without quencher (typically equal to 10^{-8} s for biomacromolecules) [51]. K_{sv} is determined from the plot

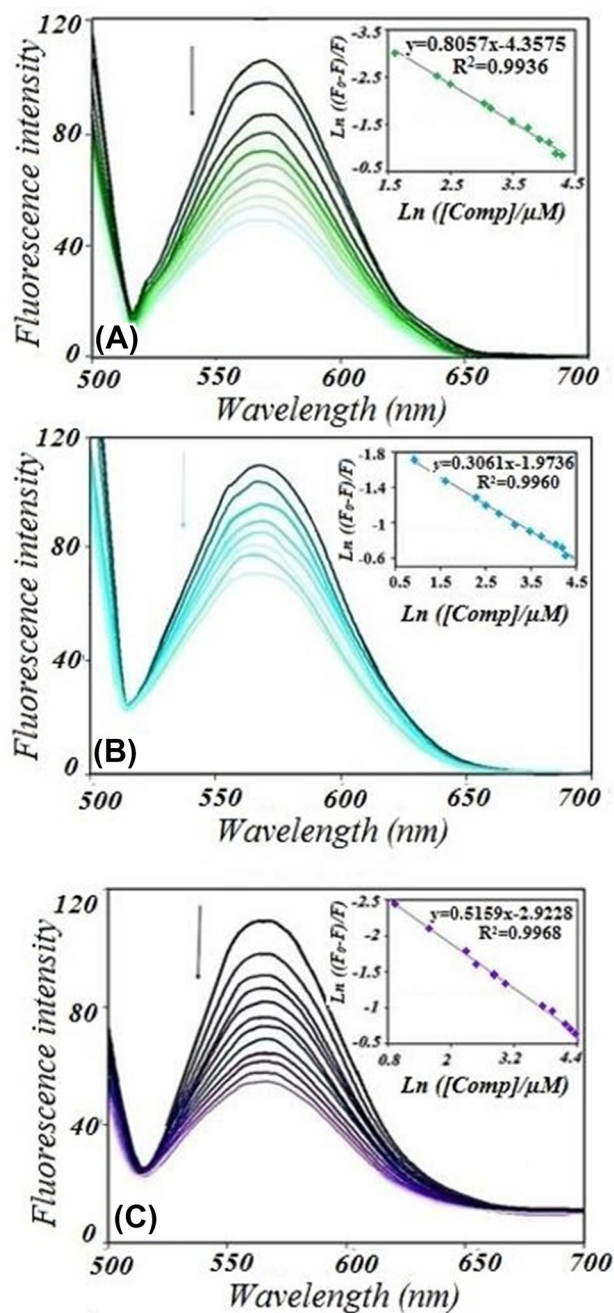


Fig. 2 Fluorescence emission spectra of EtBr–DNA system in the presence of various amounts of metal complexes: **a** Cu(II), **b** V(IV), and **c** Zn(II). [DNA] = 25 μM , [Comp] = 0–250 μM , λ_{ex} = 520 nm. K_b values were obtained from slope of the insets

of F_0/F versus. $[Q]$. The values of K_{sv} were presented in Tables 1 and 2, for HSA and DNA, respectively.

There are two mechanisms for fluorescence quenching: static quenching and dynamic quenching. In the static mechanism, the fluorophore and the quencher collide together in the ground state, but the fluorophore and quencher collide together in the excited state in dynamic mechanism [51].

The Stern–Volmer plots indicate that fluorescence quenching may have only one of the above mechanisms or combination of them [52]. Our results showed that the plots are linear, and therefore, the mechanism should be dynamic or static. The values of k_q were obtained for HSA and DNA (Tables 1 and 2, respectively), and the values were about $10^{11} \text{ M}^{-1} \text{ s}^{-1}$. This confirms that fluorescence quenching of biomolecules occurs by static mechanism, since k_q values are greater than limiting diffusion rate constant of the diffusional quenching for biopolymers ($2 \times 10^{10} \text{ M}^{-1} \text{ s}^{-1}$).

The binding constants (K_b) were determined using the following equation [52]:

$$\text{Ln}\left(\frac{F_0 - F}{F}\right) = \text{Ln}(K_b) + n\text{Ln}[Q]. \quad (2)$$

“ K_b ” is obtained from the plot of $\text{Ln}((F_0 - F)/F)$ versus $\text{Ln}[Q]$ as y-intercept. These plots are present in Figs. 1 and 2 for HSA and DNA, respectively. The K_b values (Table 1) reveal that the Zn(II)–HSA complex is more stable than the other compounds; in the other words, Zn(II)–HSA complex is more available for drug–cell interaction. Moreover, this result is in good agreement with the UV–Vis spectroscopy and molecular docking results (see Sects. “UV–Vis absorption” and “Docking study”). Furthermore, “ n ” which is the number of binding site per protein (slope of the plot) is near to 1 (Table 1), indicating that the complexes bind to HSA with molar ratio of 1:1. In general, binding constant of a drug with a carrier protein such as HSA should be high enough to bind and transfer it throughout the body. On the other hand, to release a drug in its target, K_b should not be too high. The obtained HSA-binding constants of all the complexes are in a good range ($1\text{--}6 \times 10^4$) [53]. In addition, our complexes are in uncharged form and, therefore, capable to cross through the membrane’s lipid bilayer [54]. The obtained results show that our compounds bind to HSA differently which arises from their different central metal ions and their corresponding affinities to HSA.

In addition, the binding constants (K_b) for the interaction of metal complexes with FS-DNA have been determined using Eq. (4) and are presented in Table 2. The K_b values reveal that V(IV) forms more stable complex with FS-DNA than the other complexes.

UV–Vis absorption

The UV–Vis absorption spectroscopy is also a useful technique which has been frequently used to examine binding process. The photometric titration was carried out by adding various amounts of HSA or DNA to the complexes solutions in mole ratio range of $[\text{HSA}]/[\text{complex}] = 0\text{--}4.5$ (Figs. S1 and S2). Through addition of various amounts of the HSA or DNA, a hypochromic effect was observed in the complexes

Table 1 HSA-binding constant (K_b), binding energy, the number of binding site (n), the Stern–Volmer constant (K_{SV}), and the quenching rate constant (k_q) of the metal complexes

Type of complex	$K_{\text{binding}}/\text{M}^{-1}$ (fluorescence)	$K_{\text{binding}}/\text{M}^{-1}$ (UV–Vis)	Binding energy/kcal mol ^{−1} (Molecular docking)	n	$K_{SV}/\mu\text{M}^{-1}$	$k_q/\text{M}^{-1} \text{ s}^{-1}$
Zn(II)	5.26×10^4	4.58×10^4	− 7.76	0.7978	0.0246	2.46×10^{12}
V(IV)	3.09×10^4	2.38×10^4	− 7.22	0.8336	0.0174	1.74×10^{12}
Cu(II)	1.07×10^4	5.14×10^3	− 6.98	0.9037	0.0069	6.9×10^{11}

Table 2 DNA-binding constant (K_b), binding energy, the Stern–Volmer constant (K_{SV}), and the quenching rate constant (k_q) of the metal complexes

Type of complex	$K_{\text{binding}}/\text{M}^{-1}$ (fluorescence)	$K_{\text{binding}}/\text{M}^{-1}$ (UV–Vis)	Binding energy/kcal mol ^{−1} (molecular docking)	$K_{SV}/\mu\text{M}^{-1}$	$k_q/\text{M}^{-1} \text{ s}^{-1}$
V(IV)	1.38×10^5	1.83×10^3	− 5.66	0.0069	6.9×10^{11}
Zn(II)	5.37×10^4	1.27×10^3	− 5.58	0.0059	5.9×10^{11}
Cu(II)	1.28×10^4	1.19×10^3	− 5.50	0.0060	6.0×10^{11}

absorption spectra. To assess the binding ability of the complexes with HSA and DNA, the intrinsic-binding constant (K_b) was estimated by monitoring the titration curves and using the following equation [55]:

$$\frac{1}{(\varepsilon_a - \varepsilon_f)} = \frac{1}{(\varepsilon_b - \varepsilon_f)} + \frac{1}{K_b(\varepsilon_b - \varepsilon_f)} \times \frac{1}{[\text{BM}]} \quad (3)$$

Here, [BM] is the concentration of biomacromolecule (HSA or DNA); ε_a , ε_f , and ε_b are the apparent molar absorptivity, the molar absorptivity for free compounds, and the molar absorptivity for the compounds in fully bound form, respectively. ε_f was estimated from calibration curve and ε_a is the ratio of A_{obs} to [complex]. A plot of $1/(\varepsilon_a - \varepsilon_f)$ versus $1/[\text{BM}]$ gives K_b as ratio of y-intercept to slope. The binding constants for Zn(II), V(IV), and Cu(II) complexes with HSA are about 4.58×10^4 , 2.38×10^4 , and $5.14 \times 10^3 \text{ M}^{-1}$, respectively. In the same way, binding constants for DNA–complex adducts are about 1.83×10^3 , 1.27×10^3 , and $1.19 \times 10^3 \text{ M}^{-1}$ for V(IV), Zn(II), and Cu(II), respectively.

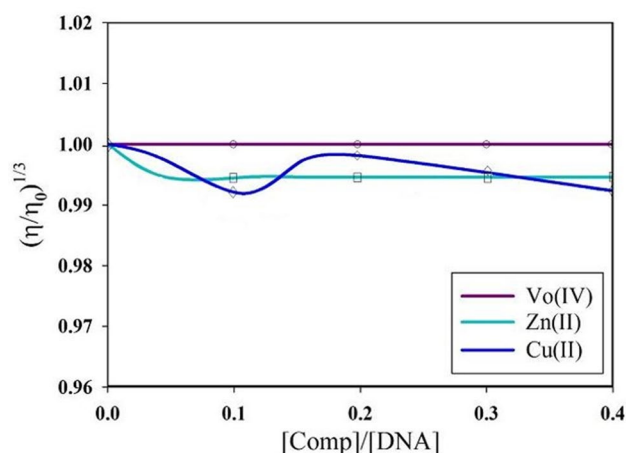
Energy transfer from HSA to the complexes

Energy transfer between the complexes and HSA can provide valuable information about HSA–complex binding. The fluorescence quenching of HSA upon its binding to metal complexes can be deduced from energy transfer between HSA and metal complexes. This energy transfer can be explained by fluorescence resonance energy transfer (FRET) theory. FRET “known as Förster’s resonance energy transfer” is an interaction between the excited molecule and its adjacent molecule, upon it; energy absorbed by donor molecule is transferred to an acceptor [56]. According to this theory, energy transfer will observe if: (1) the donor

Table 3 Obtained results from FRET theory for the metal complexes


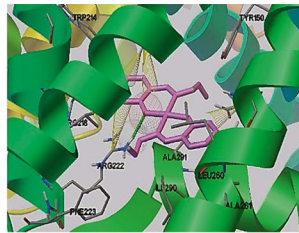
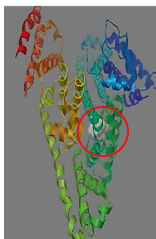
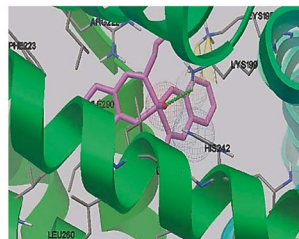

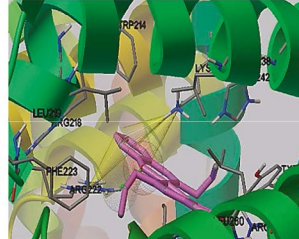
Type of complex	R_0 (nm)	r (nm)	J (cm ³ L mol ^{−1})	E
Zn(II)	3.644	4.242	1.272×10^{13}	0.286
V (IV)	3.422	4.684	8.728×10^{14}	0.132
Cu(II)	4.636	5.600	5.393×10^{13}	0.243

R_0 is the critical distance when the transfer efficiency is 50% and r is the distance between donor and acceptor. J is the overlap integral of the fluorescence spectrum of the donor with absorption spectrum of the acceptor and E is the efficiency of energy transfer (E) between tryptophan residue of protein (HSA) and drug (complex)

**Fig. 3** Effect of increasing amounts of metal complexes on the viscosity of FS-DNA. [Complex]/[DNA] = 0–0.4. [DNA] = 10 μM

has fluorescence, (2) the fluorescence emission spectrum of the donor and the UV–Vis spectrum of the acceptor have sufficient overlap, and (3) the distance between donor and

Table 4 Molecular docking results for the interaction of metal complexes with HSA

Type of complex	Amino acids around of complex	Binding site	Interactions in binding site
Zn(II)	GLU153-TYR150-ARG257- LYS199-ALA261-LEU260- ILE264-ALA291-ILE290- TRP214-ARG218-ARG222- LEU219-PHE223		
V(IV)	LYS195-TYR150-LYS199- ARG257-HIS242-LEU238- LEU260-TRP214-ILE290- ARG222-LEU219-PHE223- ILE264		
Cu(II)	TYR150-ARG257-ALA261- LEU260-ILE264-HIS242- LEU238-LYS199-ALA291- ILE290-TRP214-ARG218- ARG222-PHE223-LEU219		

acceptor is less than 8 nm [56]. The distance (r) and efficiency of energy transfer (E) between tryptophan residue of protein (HSA) and drug (complex) were calculated using this theory through the following equation:

$$E = 1 - \frac{F}{F_0} = \frac{R_0^6}{R_0^6 + r^6}, \quad (4)$$

where F_0 and F are fluorescence intensities of HSA in the absence and presence of complex, respectively. R_0 is the critical distance when the transfer efficiency is 50% and r is the distance between donor and acceptor. R_0 can be calculated by the following equation [57]:

$$R_0^6 = 8 \cdot 79 \times 10^{-25} \text{ K}^2 \text{ N}^{-4} \text{ J } \varphi. \quad (5)$$

In the above equation, the term K^2 is the orientation factor of the dipoles; N is the refractive index of medium, J is the overlap integral of the fluorescence spectrum of the donor with absorption spectrum of the acceptor, and φ is the fluorescence quantum yield of the donor. The value of J can be calculated as follows:

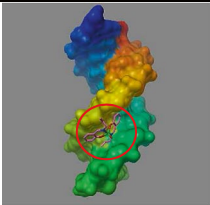
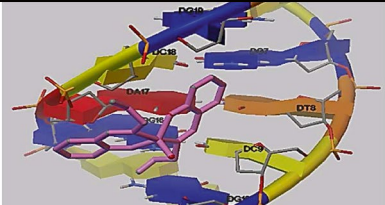
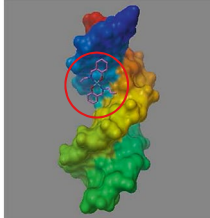
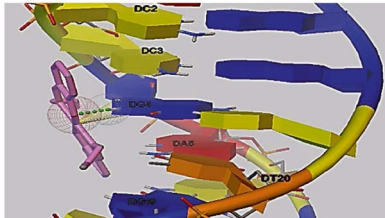
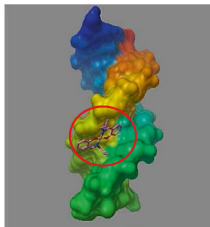
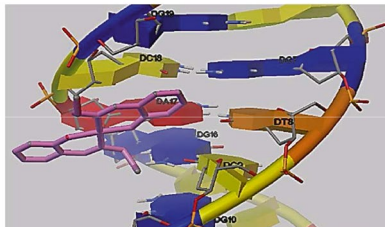
$$J = \frac{\sum F(\lambda) \varepsilon(\lambda) \lambda^4 \Delta \lambda}{\sum F(\lambda) \Delta \lambda}. \quad (6)$$

Here, $F(\lambda)$ is the fluorescence intensity of the donor in the absence of the acceptor at wavelength λ and ε is the molar absorption coefficient of the acceptor at λ . In general, $K^2 = 2/3$, $N = 1.336$ and $\varphi = 0.15$ for HSA. Therefore, according to Eqs. (4–6), the parameters for the complexes were calculated and the related results are shown in Table 3 and Fig S3. The values of r for all the complexes are less than 8 nm and $0.5 R_0 < r < 1.5 R_0$, suggesting that energy transfer from HSA to the complexes occurs with high probability.

Viscosity measurements

To further verify the interaction mode of the metal complexes with FS-DNA, viscosity measurements of DNA solution upon addition of the complexes were carried out. A classical intercalation mode causes an increase in DNA

Table 5 Molecular docking results for the interaction of metal complexes with DNA

Type of complex	Bases around of complex	Binding site	Interactions in binding site
V(IV)	DG19-DC18- DG7-DT8- DA17-DG16- DC9-DG10		
Zn(II)	DC2-DC3-DG4- DA5-DT20- DC6-DG19		
Cu(II)	DG19-DC18- DG7-DT8- DA17-DG10- DG16-DC9		

solution viscosity. This resulted from separation of base pairs by accommodated compound and subsequent increase of the DNA overall length [58]. Non-classical mode of interactions such as groove-binding and electrostatic interactions could bend the DNA helix, reduce its length, and may cause the reduction of the DNA solution viscosity [58]. The effect of the metal complexes on the viscosity of FS-DNA solution is illustrated in Fig. 3. As can be seen, the viscosity of DNA solution decreased slightly or remained constant with increasing amounts of the complexes, indicating that the binding mode of all complexes may be groove-binding. This result is in consistent with molecular docking results (Sect. “Docking study”).

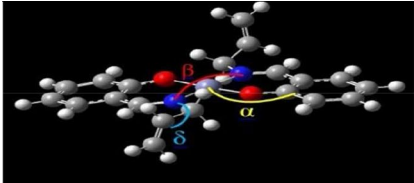
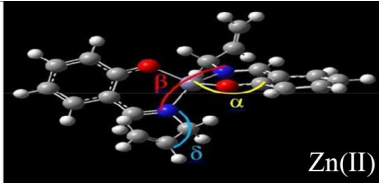
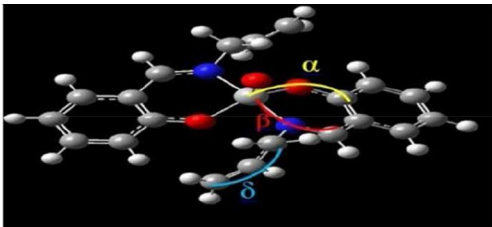
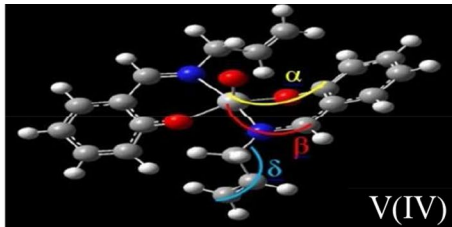
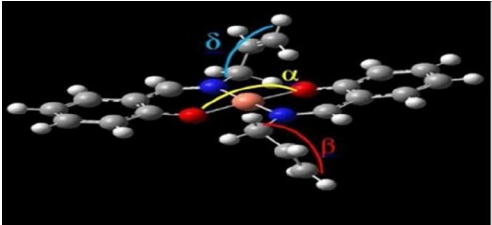
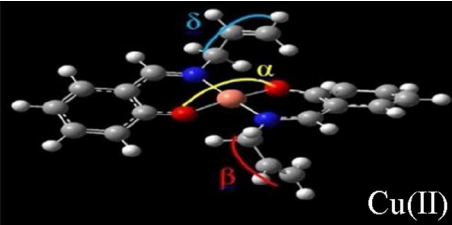
Docking study

The complexes were docked to the crystal structure of HSA and DNA. The docking results for HSA are collected in Table 4, and revealed that V(IV), Cu(II), and Zn(II) are bound to the IIA subdomain of HSA, which is the main binding site for some drugs such as thyroxine, ibuprofen, and warfarin [26]. The Cu(II) complex has hydrogen-bond interaction with Arg-222 and π -cation interactions with Arg-222 and Lys-199 residues. In addition, hydrophobic interactions with hydrophobic residues of HSA can also stabilize the

Cu(II) complex in its binding site. Furthermore, there is one hydrogen bond with Lys-199 and two π -cation with Lys-195 residue which can stabilize the V(IV) complex in its binding site. Finally, Zn(II) complex-HSA system is stabilized by one hydrogen-bond interaction with Arg-222 and four π -cation interactions with Lys-199, Arg-222, and Arg-257 residues. In addition, hydrophobic interactions have dominant role in stability of Zn(II) complex-HSA system. The obtained binding energy for all metal complex-HSA adducts are represented in Table 1. The larger negative value of binding energy for Zn(II) complex means the higher affinity for HSA binding which is in good agreement with UV-Vis and fluorescence experimental data. Moreover, the distances between Trp-214 and metal complexes were 3.151, 3.605, and 3.202 nm for Cu(II), V(IV), and Zn(II) complexes, respectively.

The docking results revealed that V(IV) and Cu(II) are bound to the minor groove of DNA. On the other hand, Zn(II) is bound to the major groove of DNA. Table 6 represents the binding mode and the nucleotides around each of metal complexes. Molecular docking results show that there are no particular interactions (such as hydrogen bond, π - π stacking, or π -cation interactions) between the Cu(II) or V(IV) complexes and nucleotides in minor groove of DNA. However, one hydrogen-bond interaction and one π -cation

Table 6 Geometry changes of the compounds during binding to HSA using ONIOM

Type of angle	Angle (before ONIOM)/degree		Angle (after ONIOM)/degree
<hr/>			
			
			
			Zn(II)
α	129.77		122.19
β	178.67		135.52
δ	111.71		117.03
<hr/>			
			
			
			V(IV)
α	131.24		111.46
β	129.21		111.06
δ	137.98		122.20
<hr/>			
			
			
			Cu(II)
α	176.47		169.45
β	111.46		115.46
δ	125.03		122.87

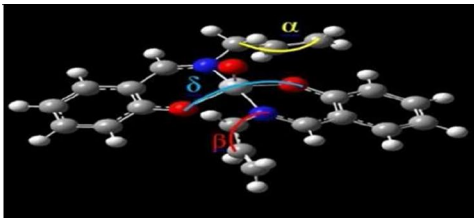
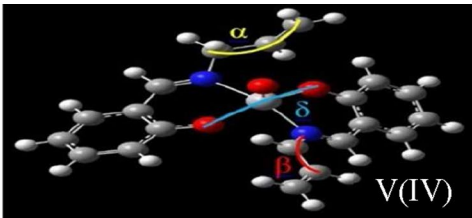
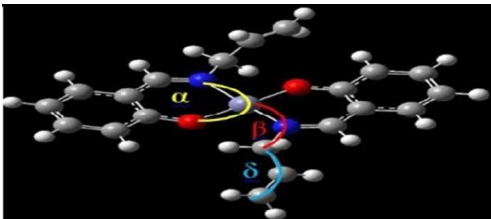
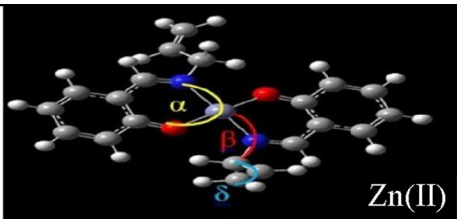
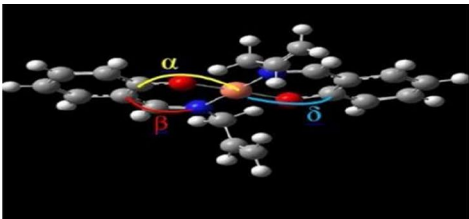
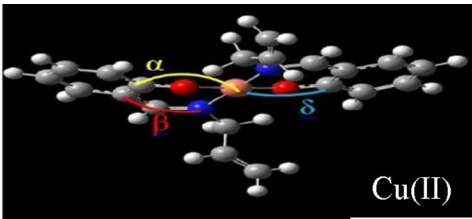
interaction with DG4 nucleotide stabilize the Zn(II) complex in the major groove of DNA. The standard binding-free energies (ΔG°), describing the affinity of the complexes for binding to DNA with the best scores, are -5.66 , -5.58 , and -5.50 kcal mol $^{-1}$ for V(IV), Zn(II), and Cu(II) complexes, respectively. The docking results are in good agreement with spectroscopic results (see Table 5). Both the experimental results and computational docking data collectively suggest that V(IV) complex has more DNA-binding affinity than the other metal complexes which it may be due to its larger structural volume than the two other ones (990.73, 967.38, and 966.75 Å 3 for V(IV), Zn(II), and Cu(II) complexes, respectively). It seems that as the structural volume of the complex increases, the orientation of the complex in the groove of DNA gets appropriate, and this can affect the fitting of the complex in the binding site. The appropriate orientation of the complex leads to the increasing of

hydrophobic interactions and the stability of DNA–complex adduct.

QM/MM calculation

In the present work, a two-layer ONIOM calculation including PM6:UFF was employed to perform QM/MM calculation. The molecular mechanics (MM) was described using the UFF force field for biomolecule (low layer), while semi-empirical quantum mechanics (QM) method (PM6) was opted for the complexes (high layer). The starting geometry of HSA–complex or DNA–complex adducts for the two-layer ONIOM study was obtained from the molecular docking simulation. The geometry was optimized using ONIOM calculation. All calculations were carried out using Gaussian 09 quantum chemistry package. The partial atomic charges on the atoms of the complexes, HSA, and DNA were used

Table 7 Geometry changes of the compounds during binding to DNA using ONIOM

Type of angle	Angle (before ONIOM)/degree	Angle (after ONIOM)/degree
<div style="display: flex; justify-content: space-around;">   </div> <div style="text-align: right; margin-right: 20px;">V(IV)</div>		
α	129.23	122.17
β	108.28	125.26
δ	127.97	143.03
<div style="display: flex; justify-content: space-around;">   </div> <div style="text-align: right; margin-right: 20px;">Zn(II)</div>		
α	92.62	90.02
β	121.45	118.02
δ	124.66	122.13
<div style="display: flex; justify-content: space-around;">   </div> <div style="text-align: right; margin-right: 20px;">Cu(II)</div>		
α	130.25	126.26
β	127.76	123.54
δ	130.11	127.48

to re-optimize the optimized geometries. The results of ONIOM indicated that structures of the complexes deviate from the initial geometry due to the binding to HSA or DNA. Along with the interaction of the complexes with HSA or DNA, some bond lengths and bond angles are changed. These changes can be resulted from the strength of the interaction between the complexes with biomacromolecules. Tables 6 and 7 show the changes in bond angles of the complexes along with binding to HSA or DNA.

Conclusion

In the current study, the binding ability of three Schiff-base metal complexes including Cu(II), V(IV), and Zn(II) to DNA or HSA was described. These metal complexes have been synthesized in our research group, previously

[34]. Herein, they were resynthesized by the same procedure and in water as a green solvent. The experimental DNA-binding results (spectroscopic and viscosity measurements) as well as computational docking and ONIOM data collectively suggest that all metal complexes interact with DNA, presumably by the groove-binding mechanism. According to this result, V(IV) complex showed stronger DNA-binding affinity than the other metal complexes which it may be due to its larger structural volume than the two other ones. Moreover, the HSA binding of the complexes was evaluated using experimental (fluorescence quenching and UV-Vis spectroscopy) and computational (molecular docking, ONIOM) methods. The obtained results indicated that the compounds bind to the IIA subdomain of HSA. The calculated binding constants between these compounds and HSA were about 1.07 to $5.26 \times 10^4 \text{ M}^{-1}$. The results of fluorescence experiment as well as the

changes in the absorption spectrum of HSA upon addition of the complexes show that the HSA–complex adducts formed in the ground state. In addition, molecular docking studies revealed that hydrogen-bond, hydrophobic, and π -cation interactions have dominant role in the binding of these complexes to HSA. In addition, the ONIOM calculation was employed to investigate the effects of the HSA interaction on geometry of the compounds. Based on the ONIOM calculations, the structural parameters of the complexes changed due to their appropriate interactions with HSA or DNA. In general, the results of the present study exhibit the effect of the metal ion on the binding of the complexes to DNA or HSA.

Acknowledgements The authors are grateful to the Research Council of the University of Isfahan for financial support of this work.

References

- Baranwal BP, Tripathi K, Singh AK, Tripathi S (2012) *Spectrochim Acta Part A Mol Biomol Spectrosc* 91:365–369
- Ershad S, Sagathforoush L-A, Karim-Nezhad G, Kangari S (2009) *Int J Electrochem Sci* 4:846–854
- Gao B, Wan M, Men J, Zhang Y (2012) *Appl Catal A Gen* 439:156–162
- Habibi MH, Shojaei E, Nichol GS (2012) *Spectrochim Acta Part A Mol Biomol Spectrosc* 98:396–404
- Bera P, Kim C-H, Seok SI (2010) *Solid State Sci* 12:532–535
- Madhu V, Sabbani S, Kishore R, Naik IK, Das SK (2015) *Cryst Eng Comm* 17:3219–3223
- Majumder I, Chakraborty P, Das S, Kara H, Chattopadhyay SK, Zangrando E, Das D (2015) *RSC Adv* 5:51290–51301
- Tian H, Yu Z, Hagfeldt A, Kloo L, Sun L (2011) *J Am Chem Soc* 133:9413–9422
- Arjmand F, Sayeed F, Muddassir M (2011) *J Photochem Photobiol B Biol* 103:166–179
- Anacona J, Rodriguez JL, Camus J (2014) *Spectrochim Acta Part A Mol Biomol Spectrosc* 129:96–102
- Sundararajan M, Jeyakumar T, Anandakumaran J, Selvan BK (2014) *Spectrochim Acta Part A Mol Biomol Spectrosc* 131:82–93
- Tarushi A, Polatoglou E, Kljun J, Turel I, Psomas G, Kessissoglou DP (2011) *Dalton Trans* 40:9461–9473
- Chakraborty A, Kumar P, Ghosh K, Roy P (2010) *Eur J Pharmacol* 647:1–12
- Joseph J, Nagashri K, Janaki GB (2012) *Eur J Med Chem* 49:151–163
- Sahani M, Yadava U, Pandey O, Sengupta S (2014) *Spectrochim Acta Part A Mol Biomol Spectrosc* 125:189–194
- Pillai SI, Subramanian SP, Kandaswamy M (2013) *Eur J Med Chem* 63:109–117
- Ki J, Mukherjee A, Rangasamy S, Purushothaman B, Song JM (2016) *RSC Adv* 6:57530–57539
- Ibrahim OB, Mohamed MA, Refat MS (2014) *Can Chem Trans* 2:108–121
- Maret W (2012) *J Inorg Biochem* 111:110–116
- Vallee BL, Auld DS (1990) *Biochemistry* 29:5647–5659
- Lu Y, Cui F, Fan J, Yang Y, Yao X, Li J (2009) *J Lumin* 129:734–740
- Cui F, Qin L, Zhang G, Liu Q, Yao X, Lei B (2008) *J Pharm Biomed Anal* 48:1029–1036
- McCallum MM, Pawlak AJ, Shadrick WR, Simeonov A, Jadhav A, Yasgar A, Maloney DJ, Arnold LA (2014) *Anal Bioanal Chem* 406:1867–1875
- Li F, Feterl M, Warner JM, Day AI, Keene FR, Collins JG (2013) *Dalton Trans* 42:8868–8877
- Domonkos C, Zsila F, Fitos I, Visy J, Kassai R, Bálint B, Kotschy A (2015) *RSC Adv* 5:53809–53818
- Ghuman J, Zunszain PA, Petitpas I, Bhattacharya AA, Otagiri M, Curry S (2005) *J Mol Biol* 353:38–52
- Bal W, Sokołowska M, Kurowska E, Faller P (2013) *Biochim et Biophys Acta Gen Subj* 1830:5444–5455
- Gou Y, Zhang Y, Qi J, Zhou Z, Yang F, Liang H (2015) *J Inorg Biochem* 144:47–55
- Kazemi Z, Amiri Rudbari H, Mirkhani V, Sahihi M, Moghadam M, Tangestaninejad S, Mohammadpoor-Baltork I (2015) *J Mol Struct* 1096:110–120
- Kazemi Z, Amiri Rudbari H, Sahihi M, Mirkhani V, Moghadam M, Tangestaninejad S, Mohammadpoor-Baltork I, Gharaghani S (2016) *J Photochem Photobiol B Biol* 162:448–462
- Khosravi I, Hosseini F, Khorshidifard M, Sahihi M, Amiri Rudbari H (2016) *J Mol Struct* 1119:373–384
- Zhang J, Zhang F, Li H, Liu C, Xia J, Ma L, Chu W, Zhang Z, Chen C, Li S (2012) *Curr Med Chem* 19:2957–2975
- Pages BJ, Ang DL, Wright EP, Aldrich-Wright JR (2015) *Dalton Trans* 44:3505–3526
- Khorshidifard M, Amiri Rudbari H, Kazemi-Delikani Z, Mirkhani V, Azadbakht R (2015) *J Mol Struct* 1081:494–505
- Pace CN, Vajdos F, Fee L, Grimsley G, Gray T (1995) *Protein Sci* 4:2411–2423
- Reichmann M, Rice S, Thomas C, Doty P (1954) *J Am Chem Soc* 76:3047–3053
- Zheng K, Liu F, Xu X-M, Li Y-T, Wu Z-Y, Yan C-W (2014) *N J Chem* 38:2964–2978
- Fu X-B, Liu D-D, Lin Y, Hu W, Mao Z-W, Le Dalton X-Y (2014) *Transactions* 43:8721–8737
- Ganeshpandian M, Loganathan R, Suresh E, Riyasdeen A, Akbarsha MA, Palaniandavar M (2014) *Dalton Trans* 43:1203–1219
- Arjmand F, Jamsheera A, Mohapatra D (2013) *J Photochem Photobiol B Biol* 121:75–85
- Fromherz P, Rieger B (1986) *J Am Chem Soc* 108:5361–5362
- Fu X-B, Weng G-T, Liu D-D, Le X-Y (2014) *J Photochem Photobiol A Chem* 276:83–95
- Waring M (1965) *J Mol Biol* 13:269–282
- Tian M-Y, Zhang X-F, Xie L, Xiang J-F, Tang Y-L, Zhao C-Q (2008) *J Mol Struct* 892:20–24
- Morris GM, Goodsell DS, Halliday RS, Huey R, Hart WE, Belew RK, Olson AJ (1998) *J Comput Chem* 19:1639–1662
- Dawson MI, Hobbs PD, Peterson VJ, Leid M, Lange CW, Feng K-C, Chen G-Q, Gu J, Li H, Kolluri SK (2001) *Cancer Res* 61:4723–4730
- Farrokhpour H, Hadadzadeh H, Darabi F, Abyar F, Amiri Rudbari H, Ahmadi-Bagheri T (2014) *RSC Adv* 4:35390–35404
- Mrkalić EM, Jelić RM, Klisurić OR, Matović ZD (2014) *Dalton Trans* 43:15126–15137
- Wang Y-Q, Zhang H-M, Zhang G-C, Tao W-H, Tang S-H (2007) *J Lumin* 126:211–218
- Dighe SU, Khan S, Soni I, Jain P, Shukla S, Yadav R, Sen P, Meeran SM, Batra S (2015) *J Med Chem* 58:3485–3499
- Darabi F, Hadadzadeh H, Ebrahimi M, Khayamian T, Amiri Rudbari H (2014) *Inorgan Chim Acta* 409:379–389
- Lakowicz JR (2006) *Plasmonics* 1:5–33
- Kyropoulou M, Raptopoulou CP, Psycharis V, Psomas G (2013) *Polyhedron* 61:126–136

54. Abou-Zied OK (2012) *Phys Chem Chem Phys* 14:2832–2839
55. Bhat SS, Kumbhar AA, Heptullah H, Khan AA, Gobre VV, Gejji SP, Puranik VG (2010) *Inorgan Chem* 50:545–558
56. Fani N, Bordbar A, Ghayeb Y (2013) *Spectrochim Acta Part A Mol Biomol Spectrosc* 103:11–17
57. Huang Y, Wang Y, Bi Y, Jin J, Ehsan MF, Fu M, He T (2015) *RSC Adv* 5:33254–33261
58. Kazemi Z, Amiri Rudbari H, Sahihi M, Mirkhani V, Moghadam M, Tangestaninejad S, Mohammadpoor-Baltork I, Azimi G, Gharaghani S, Kajani AA (2016) *J Photochem Photobiol B Biol* 163:246–260